









Article

Hydroxypropyl- β -Cyclodextrin Depletes Membrane Cholesterol and Inhibits SARS-CoV-2 Entry into HEK293T-ACE^{hi} Cells

Silvia Alboni ^{1,2,†} , Valentina Secco ^{3,†}, Bianca Papotti ⁴ , Antonietta Vilella ^{2,3} , Maria Pia Adorni ⁵ ,
Francesca Zimetti ⁴ , Laurent Schaeffer ⁶, Fabio Tascetta ^{1,2,7} , Michele Zoli ^{2,3}, Pascal Leblanc ^{6,‡} 
and Erica Villa ^{8,*} 

- ¹ Department of Life Sciences, University of Modena and Reggio Emilia, 41121 Modena, Italy; silvia.alboni@unimore.it (S.A.)
- ² Centre for Neuroscience and Neurotechnology, University of Modena and Reggio Emilia, 41121 Modena, Italy; antonietta.vilella@unimore.it (A.V.)
- ³ Department of Biomedical, Metabolic and Neural Sciences, University of Modena and Reggio Emilia, 41121 Modena, Italy
- ⁴ Department of Food and Drug, University of Parma, 43124 Parma, Italy; bianca.papotti@unipr.it (B.P.)
- ⁵ Department of Medicine and Surgery, University of Parma, 43125 Parma, Italy
- ⁶ Institut NeuroMyoGène INMG-PGNM Pathophysiology & Génétique du Neurone et du Muscle, UMR5261, Inserm U1315, 69008 Lyon, France
- ⁷ Consorzio Interuniversitario Biotecnologie (CIB), 34148 Trieste, Italy
- ⁸ CHIMOMO Department, University of Modena and Reggio Emilia, and Azienda Ospedaliero-Universitaria di Modena, 41124 Modena, Italy
- * Correspondence: erica.villa@unimore.it
- † S.A. and V.S. share first authorship.
- ‡ E.V. and P.L. share senior authorship.



Citation: Alboni, S.; Secco, V.; Papotti, B.; Vilella, A.; Adorni, M.P.; Zimetti, F.; Schaeffer, L.; Tascetta, F.; Zoli, M.; Leblanc, P.; et al.

Hydroxypropyl- β -Cyclodextrin Depletes Membrane Cholesterol and Inhibits SARS-CoV-2 Entry into HEK293T-ACE^{hi} Cells. *Pathogens* **2023**, *12*, 647. <https://doi.org/10.3390/pathogens12050647>

Academic Editor: Pawel Zmora

Received: 14 March 2023

Revised: 23 April 2023

Accepted: 24 April 2023

Published: 27 April 2023



Copyright: © 2023 by the authors. Licensee MDPI, Basel, Switzerland. This article is an open access article distributed under the terms and conditions of the Creative Commons Attribution (CC BY) license (<https://creativecommons.org/licenses/by/4.0/>).

Abstract: Vaccination has drastically decreased mortality due to coronavirus disease 19 (COVID-19), but not the rate of acute respiratory syndrome coronavirus 2 (SARS-CoV-2) infection. Alternative strategies such as inhibition of virus entry by interference with angiotensin-I-converting enzyme 2 (ACE2) receptors could be warranted. Cyclodextrins (CDs) are cyclic oligosaccharides that are able to deplete cholesterol from membrane lipid rafts, causing ACE2 receptors to relocate to areas devoid of lipid rafts. To explore the possibility of reducing SARS-CoV-2 entry, we tested hydroxypropyl- β -cyclodextrin (HP β CD) in a HEK293T-ACE^{hi} cell line stably overexpressing human ACE2 and Spike-pseudotyped SARS-CoV-2 lentiviral particles. We showed that HP β CD is not toxic to the cells at concentrations up to 5 mM, and that this concentration had no significant effect on cell cycle parameters in any experimental condition tested. Exposure of HEK293T-ACE^{hi} cells to concentrations of HP β CD starting from 2.5 mM to 10 mM showed a concentration-dependent reduction of approximately 50% of the membrane cholesterol content. In addition, incubation of HEK293T-ACE^{hi} cells with HIV-S-CoV-2 pseudotyped particles in the presence of increasing concentrations of HP β CD (from 0.1 to 10 mM) displayed a concentration-dependent effect on SARS-CoV-2 entry efficiency. Significant effects were detected at concentrations at least one order of magnitude lower than the lowest concentration showing toxic effects. These data indicate that HP β CD is a candidate for use as a SARS-CoV-2 prophylactic agent.

Keywords: SARS-CoV-2; cyclodextrin; lipid raft; cholesterol; prophylaxis

1. Introduction

Coronavirus disease 19 (COVID-19) is a severe infectious disease caused by a recently discovered coronavirus family member, SARS-CoV-2 (severe acute respiratory syndrome coronavirus 2) [1]. Since its first identification in 2019 in China, it has spread worldwide, resulting in the COVID-19 pandemic.

Mortality rates were initially very high, but in late 2020, different types of vaccines for COVID-19 became available. Their extensive use has led to a notable change in the clinical scenario. Mortality rates have drastically reduced, and the severity of the clinical picture has generally improved.

However, despite a full course of vaccination, a considerable proportion of subjects still contract the infection [2]. Furthermore, secondary attack rates for household contacts exposed to fully vaccinated index cases with acute SARS-CoV-2 infection were similar to household contacts exposed to unvaccinated index cases [3]. In addition, approximately 40% of infections in fully vaccinated household contacts arise from fully vaccinated epidemiologically linked index cases [3]. Although breakthrough infections are common, their number in a typical crowded environment is not high. The isolation of infectious virus from the nasopharynx of vaccinated individuals indicates a possible route of infection [4].

This can be further aggravated by the varying infectivity of the various SARS-CoV-2 strains. It has been estimated that each person infected with the Delta strain can infect 3–5 people they come into contact with. However, for the newer strains such as Omicron, there is evidence that infectivity is much higher. One person with Omicron could transmit the virus to approximately 20 others [5,6]. Recently isolated Omicron variants such as XBB.1.16, which was associated with the epidemic surge in India, are potentially even more infectious [7].

To date, there are no prophylactic measures that can be applied to lower the risk of acquiring the infection for people who, for several reasons, may be at high risk despite vaccination. In this regard, a possible strategy could be to hinder the entry of SARS-CoV-2 into the nasal or pharyngeal mucosa by using a substance that would prevent viral spike protein from combining with membrane receptors. The main receptor for SARS-CoV-2 is the angiotensin-I-converting enzyme 2 (ACE2) receptor, which is present in both the respiratory and digestive systems, with an increasing concentration from the upper to the lower digestive system. SARS-CoV-2 infection initiates with the interaction of the spike protein localized on the virus envelope with the ACE2 receptor. A generic way of interfering with the mechanism of entry of SARS-CoV-2 into cells could exploit the modification of the binding capacity of the ACE2 receptor with the spike protein. The ACE2 receptors are located in microdomains of the cell membrane known as lipid rafts, which are rich in cholesterol and sphingolipids. Depletion of cholesterol from the cell membrane through various treatments results in profound modifications, including the relocalization of ACE2 receptors to areas devoid of lipid rafts, leading to a 90% reduction in SARS-CoV-2 infectivity in cell lines [8]. Cyclodextrins (CDs) are one of the most efficient groups of substances for achieving cholesterol depletion in cell membranes. Among these, hydroxypropyl- β -cyclodextrin (HP β CD), has been extensively studied. Several *in vivo* and *in vitro* studies have demonstrated low toxicity of this molecule [9], even when administered intravenously, both in animal models [10] and in humans [11].

In our study, we aimed to verify whether HP β CD could interfere with the entry of SARS-CoV-2 into cells, and whether this could lead to a decrease in its infectivity. To explore this possibility, we used a HEK293T-ACE2^{hi} cell line that stably overexpressed human ACE2 and SARS-CoV-2 Spike-pseudotyped lentiviral particles.

2. Materials and Methods

2.1. Cells

The human embryonic kidney cells (HEK293T) used in this study were obtained from the ATCC. The HEK293T-ACE2^{hi} cell line was engineered to stably overexpress human ACE2 tagged with a hemagglutinin HA flag. Briefly, HEK293T cells were plated at a density of 400,000 cells per well (6-well plate) one day before transfection with 2 μ g of pCMV3-ACE2-HA-Hygro encoding construct using the Fugène HD transfection reagent according to the manufacturer's protocol (Promega, Milan, Italy). One day after transfection, the cells were treated with hygromycin, and selection was completed once non-transfected HEK293T control cells were fully stained.

Cells were cultured in Dulbecco's modified Eagle medium (DMEM) supplemented with 10% fetal bovine serum (FBS), 2 mM L-Glutamine, and 0.1 mg/mL of penicillin/streptomycin at 37 °C in a humidified atmosphere of 5% CO₂ in air. All of the reagents used to culture the cells were purchased from Merck KGaA, Darmstadt, Germany. For the experiments, ~80% confluent cultures were harvested and maintained in complete medium for 24 h. before treatment.

2.2. Drugs

HPβCD was purchased from Wacker Chemie, and α-cyclodextrin (αCD) was purchased from Merck KGaA, Darmstadt, Germany. HPβCD and αCD solutions were freshly prepared and dissolved in HEK293T-ACE^{hi} cell medium (vehicle).

2.3. Cytotoxicity Assay

Cell viability was evaluated using the MTT assay to measure cellular metabolic activity as an indicator of cell viability. HEK293T-ACE^{hi} cells were seeded at a concentration of 10⁴ cells/well in 100 μL of complete medium with 10% FBS into 96-well plates. One day post-seeding, a vehicle or HPβCD (concentration range 0.01–40 mM) were added and tested for overnight incubation, followed by a 4 h incubation with a Thiazolyl Blue Tetrazolium Bromide (MTT; Merck KGaA, Darmstadt, Germany) solution (5 mg/mL) at 37 °C in a humidified 5% CO₂/air atmosphere. The formazan formed was dissolved in 150 μL acid isopropanol (0.1 N HCl in isopropanol) added to all wells. The absorbance was measured by a multiplate reader at a 570 nm wavelength with a 620 nm reference wavelength. All experiments were performed twice ($n = 8$ for each experiment) in independent cultures. The results were expressed as a percentage of the controls.

2.4. Cell Cycle Analysis

The analysis of the cell cycle using flow cytometry was performed to investigate the potential cytotoxicity of HPβCD based on the quantification of cellular DNA content using a fluorescent DNA-selective stain, propidium iodide (PI), that exhibits emission signals proportional to DNA mass. HEK293T-ACE^{hi} cells were seeded in a 24-well plate (75,000 cells/well) in a complete medium at 37 °C in 5% CO₂. After 24 h post-seeding, cells were treated overnight with 5 or 20 mM HPβCD or a vehicle. The cell cycle analysis was carried out immediately after 24 h, or 72 h after the overnight HPβCD treatment to evaluate whether HPβCD can affect the cell cycle stages over time.

After the treatment or recovery, cells were collected by trypsinization, pelleted by centrifugation for 5 min at 200× *g*, and then resuspended in ice-cold PBS. To permeabilize the samples, 50 μg/mL of RNase A and 50 μg/mL PI staining solution with 0.1% Triton X-100 were added for 20 min at 4 °C in the dark. After incubation, flow cytometry was performed to determine the cell cycle distribution using an Attune NxT Acoustic Focusing Cytometer (Thermo Fisher Scientific, Monza, Italy).

2.5. Plasma Membrane Cholesterol Content

Plasma membrane oxidase-sensitive cholesterol was quantified using a radioisotopic assay as previously described [12]. Briefly, HEK293T-ACE^{hi} cells, 48 h after seeding, were incubated with 3 μCi/mL (1-2,3) of cholesterol (Perkin Elmer, MA, USA) for 24 h in the presence of 2 μg/mL of an acyl-coenzyme A, a cholesterol acyltransferase (ACAT) inhibitor (Sandoz 58035; Merck, Germany), to ensure that all cholesterol was in the free form. Cells were then treated for 18 h with increasing concentrations of HPβCD (from 0.01 mM to 15 mM) or a vehicle, along with 2 μg/mL of ACAT inhibitor. The culture medium was then removed, and cholesterol oxidase enzyme from *Streptomyces* (Merck, Darmstadt, Germany) dissolved in PBS was added at a concentration of 1 U/mL for 2 h at 37 °C. The PBS was then removed, lipids were extracted from the cell monolayers after 18 h of incubation with 2-propanol, and thin layer chromatography (TLC) was performed to separate radioactive free, esterified, and oxidated cholesterol within the extracted lipid

fraction (the mobile phase was composed of 90 mL hexane, 10 mL ethyl ether, and 1 mL methanol). The plasma membrane cholesterol content was expressed as the percentage of oxidated cholesterol over the total cholesterol. In parallel, the total protein content was quantified in cell monolayers using the bicinchoninic acid assay (BCA; Thermo Fisher Scientific, MA, USA) following the manufacturer's instructions. All experiments were performed twice ($n = 5-9$) in independent cultures.

2.6. Plasmids

The FUGW-GFP construct encodes the gene for GFP that has been cloned into the lentivirus plasmid FUGW. This construct was kindly provided by Dr. Xandra O. Breakefield [13]. The psPAX2 plasmid, a second-generation lentiviral packaging construct encoding the HIV-1 Gag, GagPol, Tat, and Rev accessory proteins, was kindly provided by Dr. Didier Trono (EPFL). The pCG1-Spike-HA construct encoding the Wuhan SARS-CoV-2 Spike Envelope glycoprotein was kindly provided by Dr Stefan Pölmann [14] and the pCMV3-2019-nCoV-Spike(S1+S2)-long Flag and untagged (VG40589-CF and VG40589-UT) were purchased from Sino Biological Europe GmbH (Eschborn, Germany).

2.7. Pseudotyped Lentiviral Particles Production

Lentivector particles were produced by calcium phosphate DNA transfection of HEK293T cells with the HIV-1 packaging construct pSPAX2, the miniviral genome bearing the expression cassette encoding GFP (FUGW-GFP), and the plasmid encoding either the SARS-CoV-2 Spike Envelope glycoproteins or the VSVg envelope expressing plasmid pMD2.G (addgene). Lentivector particles were also produced without the viral entry glycoprotein as a negative control. For vector production, packaging, transfer, and envelope encoding, plasmids were transfected at a ratio of 8:8:4 μg for 3.5×10^6 cells plated 1 day before transfection in 100 mm dishes. Lentivectors were recovered from the cell culture supernatant 48 h after transfection, centrifuged at $3000 \times g$ for 5 min, filtrated (0.45 μm filter, Millipore, Burlington, MA, USA), aliquoted, and stored at -80°C until use.

2.8. Single-Cycle Infectivity Assay

HEK293T-ACE^{hi} cells (75,000 cells/well) were seeded in a 24-well plate and cultured in complete medium (w/o antibiotics) at 37°C in 5% CO_2 overnight. Twenty-four hours post-seeding, cells (untreated or treated with HP β CD; concentration range from 0.1 to 10 mM) were incubated with 200 μL of pseudotyped viral particles overnight. Over the next three days, cells were washed twice with PBS and maintained in culture with 1 mL of complete medium at 37°C in 5% CO_2 . After 72 h post-infection, GFP expression was qualitatively evaluated using EVOS Cell Imaging Systems (Thermo Fisher Scientific) and quantitatively evaluated using cytofluorimetry with an Attune NxT Acoustic Focusing Cytometer (Thermo Fisher Scientific) to determine infection efficiency. Three independent experiments were performed ($n = 5-9$).

2.9. Curve Fit and Statistical Analysis

The CD concentrations were converted to Log10 values, and curve fit and IC50 values were calculated using the Nonlinear regression One site—Fit logIC50 function of the Prism software, version 7 (GraphPad Software, San Diego, CA, USA). Statistical significance was assessed by one-way analysis of variance (ANOVA) and post-hoc Dunnett's test for multiple comparisons against the control (vehicle-exposed) group. A value of $p < 0.05$ was considered statistically significant. All data are presented as mean \pm standard error of mean (SEM). Statistical analysis was performed using Prism statistical analysis software, version 7 (GraphPad Software, CA, USA) or SPSS for Windows v.28 (SPSS Inc., Chicago, IL, USA).

3. Results

3.1. HP β CD Concentration-Dependent Effects on Cell Viability and Cell Cycle

Although HP β CD has been reported to exhibit high biocompatibility, we first evaluated the cytotoxic effects of overnight exposure to HP β CD (concentration range from 0.01 to 40 mM) or a vehicle (Ctrl) on HEK293T-ACE^{hi} cells. The analysis revealed a concentration-dependent effect of HP β CD exposure on cell viability in HEK293T-ACE^{hi} cells (one-way ANOVA: $F(9,151) = 73.007$, $p < 0.001$, followed by post-hoc Dunnett's test). HP β CD was not found to be toxic up to a concentration of 5 mM ($p = 0.964$). Higher concentrations were increasingly toxic, with a 40 mM concentration of HP β CD resulting in extreme toxicity (reduction of cell viability by ~90%; $p < 0.001$ vs. Ctrl) (Figure 1).

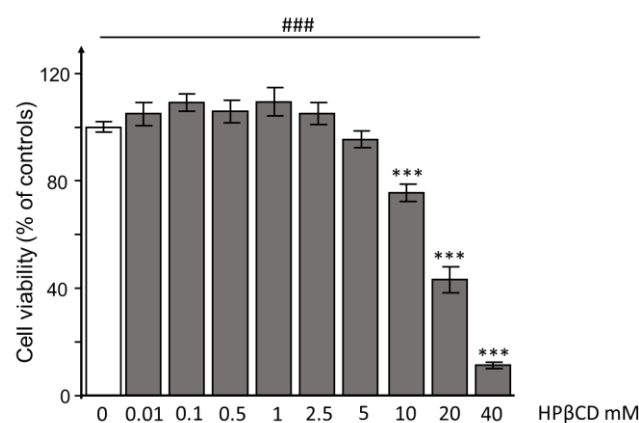


Figure 1. Hydroxypropyl- β -cyclodextrin does not induce cytotoxic effects in HEK293T-ACE^{hi} cells up to a concentration of 5 mM. HEK293T-ACE^{hi} cells were treated overnight with 0.01, 0.1, 0.5, 1, 2.5, 5, 10, 20, or 40 mM of HP β CD (grey columns) or a vehicle (0; white column) and then tested for cell viability (MTT test). Data are the mean \pm SEM of two independent experiments ($n = 8$ for each experiment). The concentration effect of HP β CD on cell viability was determined with a one-way ANOVA (### $p < 0.001$) followed by a post-hoc Dunnett's test vs. control (** $p < 0.001$). HP β CD: hydroxypropyl- β -cyclodextrin.

It has been reported that HP β CD is less toxic than other CDs (including the parent β -cyclodextrins, β CDs) (9). We used the same experimental conditions to evaluate the cytotoxic effects induced by α CD, which is able to extract cholesterol from membranes, although to a lesser extent than HP β CD. We demonstrated that overnight exposure to α CD at concentrations of 2.5 or 5 mM resulting in different effects than those observed for HP β CD (see above). The significant reduction in cell viability was demonstrated through a one-way ANOVA, which showed $F(2,23) = 17.974$, $p < 0.001$ vs. control, followed by a post-hoc Dunnett's test (Figure S1).

In leukemic cell lines, HP β CD inhibits cell growth by reducing intracellular cholesterol and inducing G2/M cell-cycle arrest [15], showing that this CD can affect the cell cycle. We then evaluated HP β CD-induced effects on the cell cycle of HEK293T-ACE^{hi} immediately, 24 h, or 72 h after overnight exposure (concentrations: 5 or 20 mM). One-way ANOVA analysis revealed a significant effect on the percentage of cells in the G0/G1 phase ($F(2,25) = 16.951$, $p < 0.001$) and the G2/M phase ($F(2,25) = 3.790$, $p = 0.038$) immediately after overnight exposure only at the highest concentration of HP β CD tested (20 mM). This concentration increased the percentage of cells in the G2/M phase ($p = 0.044$, post-hoc Dunnett's test), while decreasing the percentage of cells in G0/G1 ($p < 0.001$, post-hoc Dunnett's test). In the same experimental conditions, the proportion of S-phase cells was not significantly affected by HP β CD (Figure 2a). The effect of 20 mM HP β CD on the HEK293T-ACE^{hi} cell cycle was reversible since it had no effect on the HEK293T-ACE^{hi} cell cycle 24 or 72 h after overnight exposure (Figure 2b,c). A concentration of 5 mM of HP β CD had no significant effect on the cell cycle parameters in any experimental condition tested

(Figure 2a–c). The percentage of apoptotic cells was not significantly affected by HP β CD treatments at 24 or 72 h or immediately after an overnight exposure (Figure 2).

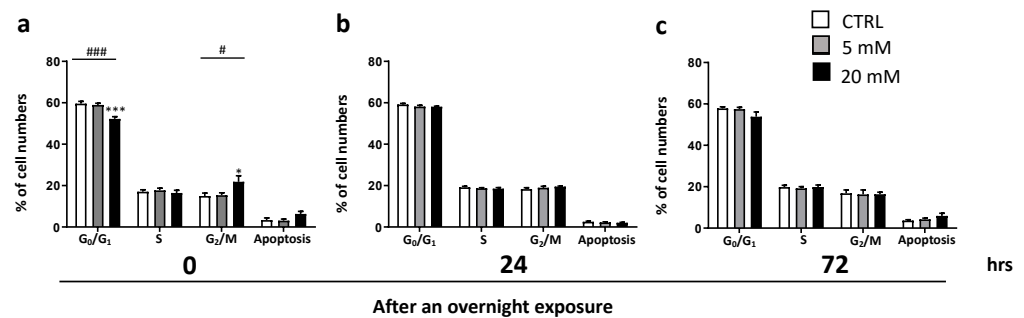


Figure 2. A concentration of 20 mM, but not 5 mM, of hydroxypropyl- β -cyclodextrin transiently affects cell cycle after overnight exposure without significant effect on apoptosis. HEK293T-ACE^{hi} cells were treated overnight with 5 or 20 mM HP β CD or a vehicle (control) and tested for cell cycle distribution analysis using flow cytometry (a) immediately after, (b) 24 h after, or (c) 72 h after HP β CD or a vehicle treatment. Histograms show the percentage of cells in the G₀/G₁, S and the G₂/M phase. Data are presented as the mean \pm SEM of two independent experiments ($n = 5-9$). The concentration effect of HP β CD on each cell cycle phase was determined by one-way ANOVA (# $p < 0.05$, ### $p < 0.001$) followed by post-hoc Dunnett's test vs. controls (* $p < 0.05$, *** $p < 0.001$). HP β CD: hydroxypropyl- β -cyclodextrin. White columns: control; grey columns: 5mM HP β CD; black columns: 20 mM HP β CD.

Overall, our experiments did not show evidence of HP β CD-induced cell toxicity or cell cycle alterations for concentrations up to 5 mM.

3.2. HP β CD Effects on Membrane Cholesterol Content

Cholesterol, and in particular its distribution in membrane rafts, is essential for viral interaction with ACE2 receptors and entry into the cell [16]. Therefore, we evaluated the modulating effect of increasing concentrations of HP β CD with overnight exposure on the membrane cholesterol content of HEK293T-ACE^{hi} cells. The analysis revealed a concentration-dependent reduction of approximately 50% of the initial membrane ³H-cholesterol content induced by HP β CD exposure in HEK293T-ACE^{hi} cells (one-way ANOVA: $F(7,58) = 18.627$; $p < 0.001$, followed by post-hoc Dunnett's test, Figure 3a). In particular, a significant reduction in membrane ³H-cholesterol content was induced by HP β CD exposure starting from 2.5 mM and reaching the maximum inhibitory effect at 10 mM. The concentration-response inhibition curve showed an IC₅₀ value of 1.99 mM (Figure 3b).

3.3. HP β CD Effects on Pseudotyped SARS-CoV-2 Particle Entry into HEK293T-ACE2^{hi} Cells

Lentiviral particles that were pseudotyped with SARS-CoV-2 Spike Envelope glycoprotein (HIV-S-CoV2) have been repeatedly used to investigate SARS-CoV-2 entry mechanisms [17,18]. HEK293T-ACE^{hi} cells were incubated overnight with HIV-S-CoV2 pseudotyped particles in the presence of increasing concentrations of HP β CD (from 0.1 to 10 mM) or a vehicle and maintained in culture for 72 h. Three days post-incubation, GFP expression was qualitatively evaluated using EVOS Cell Imaging Systems and quantitatively evaluated using cytofluorimetry to determine the viral particles' entry efficiency. The analysis revealed a concentration-dependent effect of HP β CD exposure on entry efficiency (one-way ANOVA: $F(6,41) = 222.178$, $p < 0.001$, followed by post-hoc Dunnett's test) (Figure 4a–c), with clearly significant effects detected at concentrations at least one order of magnitude lower than the lowest concentration showing toxic effects (see above). The concentration-response inhibition curve showed an IC₅₀ value of 0.78 mM.

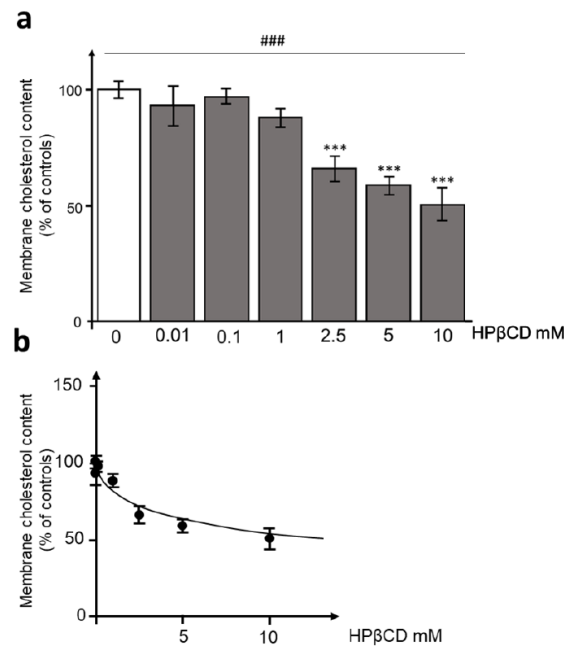


Figure 3. Hydroxypropyl-β-cyclodextrin concentration dependently reduces membrane ³H-cholesterol content in HEK293T-ACE^{hi} cells. HEK293T-ACE^{hi} cells were radiolabeled with [³H] cholesterol for 24 h and treated with HPβCD with concentrations ranging from 0.01 to 15 mM (or a vehicle) for an additional 18 h, as described in the Methods. Cholesterol oxidase [1 U/mL] was then incubated for 2 h to oxidize the cholesterol fraction selectively present in cell membranes. Membrane cholesterol content was calculated by counting the radioactivity of oxidized cholesterol over the total cellular radioactive cholesterol. In panel (a), the results are reported as the percentage of membrane cholesterol content in HPβCD-treated cells compared to vehicle-treated (control) cells. In panel (b), the concentration–response curve was fitted using the Nonlinear regression One site—Fit logIC50 function of the Prism software to obtain the IC50 value. Data are expressed as means ± SEM (*n* = 4 per group). A one-way ANOVA (### *p* < 0.001) followed by the post-hoc Dunnett’s test (***) (*p* < 0.001 vs. vehicle-treated cells) was used to analyze the differences between the experimental conditions.

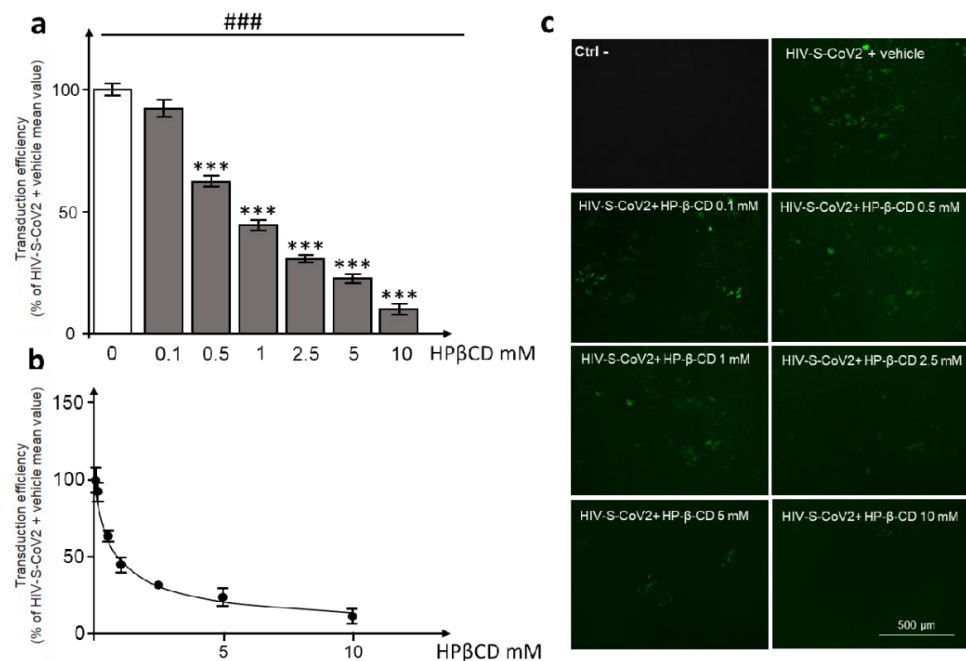


Figure 4. Hydroxypropyl-β-cyclodextrin concentration dependently reduces lentiviral particles pseudotyped with SARS-CoV-2 Spike Envelope glycoprotein entry into HEK293T-ACE^{hi} cells. HEK293T-

ACE^{hi} cells were incubated with pseudotyped viral particles containing a GFP expression cassette overnight in the presence of different concentrations (0.1 to 10 mM) of HP β CD or a vehicle. Cells were also incubated overnight with lentivector particles without viral entry glycoprotein containing a GFP expression cassette as a negative control (Ctrl-). Three days post-transduction, (a) GFP expression was measured by flow cytometry and (b) the concentration–response curve was fitted using the Nonlinear regression One site—Fit logIC₅₀ function of the Prism software to obtain the IC₅₀ value. Qualitative analysis (c) was performed using EVOS Cell Imaging Systems Panel on live-HEK293T-ACE^{hi} cells before proceeding to the quantitative analysis. Scale bar = 500 μ m. Data are expressed as means \pm SEM ($n = 3$ –11, three independent experiments). A one-way ANOVA (### $p < 0.001$) followed by the post-hoc Dunnett's test (** $p < 0.001$ vs. vehicle treated cells) was used to analyze the differences between the experimental conditions.

As a positive control for viral entry, we performed experiments with HIV-VSVg pseudo-particles. No significant effect on their entry was observed after the modestly cytotoxic 10 mM HP β CD dose (one-way ANOVA: $F(2,37) = 21.582$, $p < 0.001$, followed by post-hoc Dunnett's test) (see Figure S2).

4. Discussion

The main finding of this study is that HP β CD, at concentrations that are neither cytotoxic nor interfere with cell cycle, markedly reduces (down to approximately 22%) the entry of pseudotyped SARS-CoV-2 particles into HEK293T cells stably overexpressing human ACE2 (HEK293T-ACE^{hi} cells). Pseudotyped HIV-1 lentiviral particles with the SARS-CoV-2 Spike Envelope glycoprotein are widely used to study molecular and cellular mechanisms of SARS-CoV-2 entry [17,18], allowing recognition of the principal membrane receptors and associated proteins necessary for virus entry.

We also demonstrated that HP β CD can decrease membrane ³H-cholesterol content by approximately 50%. Remarkably, the IC₅₀ values of the HP β CD-induced decrease in HIV pseudotyped SARS-CoV-2 Spike particle entry and the membrane cholesterol content were close to each other, both at approximately 1 mM. The first effective concentration of HP β CD was close to one order of magnitude below its lowest cytotoxic concentration. Therefore, our hypothesis is that HP β CD-induced decrease in membrane cholesterol content leads to a disruption in membrane organization; more specifically, the cholesterol-rich lipid rafts where many known SARS-CoV-2 receptors are located [16], thus hindering the processes of viral entry into the cell.

Lipid rafts are microdomains of the cell membrane that are rich in cholesterol, sphingolipids, and proteins. This lipid composition causes the membrane to acquire greater rigidity, making it an ideal platform for several receptors including ACE2 [16,19,20]. These structures are critical for coronaviruses, including SARS-CoV-1, to enter into cells and maintain infectivity [8]. Cholesterol depletion in the cell membrane, regardless of the method used, causes profound changes in the membrane's physical properties [21] and induces the re-localization of receptors localized in the lipid rafts, including ACE2, to areas without lipid drafts [16]. Of further interest is the fact that not only ACE2, but also several other co-receptors that are relevant for SARS-CoV-2 binding and internalization such as heparan sulfate proteoglycan [22], Syndecan-1/4 [23], Neuropilin-1 [24], L-SIGN [25], HDL scavenger receptor B type 1 [26], CD147 [27], and human Toll-like receptors [28] are abundant in the lipid rafts [16]. This means that HP β CD can perturb SARS-CoV-2 binding not only to ACE2 but also to all the other co-localized co-receptors, thus strengthening the inhibitory effect of HP β CD on virus entry.

Another relevant consequence of this putative mechanism of action is that it is variant-independent. This is because the interference with the binding and internalization of SARS-CoV-2 is primarily related to a physical disturbance of the cellular membrane. This is particularly relevant in view of the extremely rapid appearance of SARS-CoV-2 variants

with the accumulation of a huge number of mutations that can weaken vaccine protection [29,30].

The motivation for our study was to search for a substance that could be used as a prophylaxis for SARS-CoV-2 infection. This substance would need to be easily delivered to the site of entry of the virus, i.e., the nasal and oropharyngeal mucosa. CDs were identified as ideal candidates due to their longstanding experience in intranasal delivery as carriers of scarcely soluble drugs, showing their safety and ease of use [31,32]. All types of CDs, including α CDs, β CDs, and γ -cyclodextrins (γ CDs), can extract cholesterol from cell membranes and disrupt lipid rafts, although with different efficiencies depending on the size and hydrophobicity of their inner cavity [33]. However, α CDs are more efficient in extracting phospholipids than cholesterol [34] and are toxic to cells even at low concentrations, and γ CDs are not sufficiently hydrophobic [34,35]. β CDs have the best characteristics to exert this protective action. Among the β CDs, methyl β CD (M β CD) and HP β CD are those that have been most studied. Their *in vitro* activity for cholesterol depletion is similar, as well as their solubility, due to hydrophilic modifications (such as methylation and hydroxypropylation).

Lu et al. were among the first to test M β CD in the context of SARS-CoV infection [8], while Li et al. evaluated the role of M β CD to inhibit SARS-CoV-2 infection *in vitro* [17]. We used a similar approach, but chose to evaluate HP β CD instead. For the purpose of using CDs as SARS-CoV-2 prophylaxis, M β CD did not meet our requirements. This was because, in the direct comparison between HP β CD and M β CD, the latter was shown to be significantly more toxic both *in vitro*, even at very low concentrations [36,37], and *in vivo* [38]. More specifically, the latter study showed that the outer hair cells (OHC) in the organ of Corti appeared histologically normal after treatment with 13 mM of HP β CD, while a higher concentration (27 mM) only caused sporadic damage. Instead, 13 mM of M β CD caused severe damage to the OHC [37]. Notably, in our study, the most effective concentration of HP β CD that was able to inhibit pseudotyped SARS-CoV-2 particle infection (5 mM) was approximately five times lower than the mildly toxic concentration tested in [38]. During the course of our study, a relevant study by Bezerra et al. [39] was published. These authors used experimental models that were partially different from ours (native VERO cells and VERO E6 expressing Transmembrane Protease Serine 2 and Human Angiotensin-Converting Enzyme 2; Calu3 and, as in our study, ACE2 transfected 293T) and showed that HP β CD primarily reduces virus replication and the release of infectious SARS-CoV-2 particles rather than inhibiting entry into the cells. Treatment of human primary monocytes with HPBCD also reduced inflammatory cytokines. Although some relevant experimental conditions were different (e.g., HP β CD was used at much higher concentrations than in the present study), these data are complementary to our findings and indicate an interesting therapeutic potential for this compound.

5. Conclusions

In conclusion, data on the ability of HP β CD to interfere with SARS-CoV-2 infection is accumulating, making it a strong candidate as a prophylactic agent.

Supplementary Materials: The following supporting information can be downloaded at: <https://www.mdpi.com/article/10.3390/pathogens12050647/s1>, Figure S1: α -cyclodextrin induces cytotoxic effect in HEK293T-ACEhi cells.; Figure S2: A 20 mM dose of hydroxypropyl- β -cyclodextrin (HP β CD) reduces entry of lentiviral particles pseudotyped with VSVg Envelope glycoprotein into HEK293T-ACEhi cells.

Author Contributions: Conceptualization, S.A. and E.V.; data curation, S.A. and V.S.; formal analysis, S.A., V.S., B.P., A.V., M.P.A., F.Z. and L.S.; funding acquisition, E.V.; investigation, B.P. and A.V.; methodology, A.V. and M.Z.; project administration, E.V.; resources, P.L.; supervision, S.A., F.T., M.Z. and E.V.; validation, M.P.A.; writing—original draft, S.A. and E.V.; writing—review and editing, S.A., B.P., M.P.A., F.Z., L.S., F.T., M.Z., P.L. and E.V. All authors have read and agreed to the published version of the manuscript.

Funding: This research was supported by grants from Regione Emilia-Romagna Bankitalia (PG-2020-252325) to E.V.; MIUR Dipartimenti di Eccellenza 2018–2022 to M.Z., A.V., V.S., and French ANR Flash COVID-19 Acoustovie ANR-20-COVI-0080 to P.L.

Institutional Review Board Statement: Not applicable.

Informed Consent Statement: Not applicable.

Data Availability Statement: All data generated and analyzed throughout the current study are available from the corresponding author upon reasonable request.

Conflicts of Interest: The authors declare no conflict of interest.

References

1. Zhu, N.; Zhang, D.; Wang, W.; Li, X.; Yang, B.; Song, J.; Zhao, X.; Huang, B.; Shi, W.; Lu, R.; et al. A Novel Coronavirus from Patients with Pneumonia in China. *N. Engl. J. Med.* **2020**, *382*, 727–733. [[CrossRef](#)] [[PubMed](#)]
2. Di Fusco, M.; Moran, M.M.; Cane, A.; Curcio, D.; Khan, F.; Malhotra, D.; Surinach, A.; Miles, A.; Swerdlow, D.; McLaughlin, J.M.; et al. Evaluation of COVID-19 vaccine breakthrough infections among immunocompromised patients fully vaccinated with BNT162b2. *J. Med. Econ.* **2021**, *24*, 1248–1260. [[CrossRef](#)] [[PubMed](#)]
3. Singanayagam, A.; Hakki, S.; Dunning, J.; Madon, K.J.; Crone, M.A.; Koycheva, A.; Derqui-Fernandez, N.; Barnett, J.L.; Whitfield, M.G.; Varro, R.; et al. Community transmission and viral load kinetics of the SARS-CoV-2 delta (B.1.617.2) variant in vaccinated and unvaccinated individuals in the UK: A prospective, longitudinal, cohort study. *Lancet Infect. Dis.* **2022**, *22*, 183–195. [[CrossRef](#)]
4. Hagan, L.M.; McCormick, D.W.; Lee, C.; Sleweon, S.; Nicolae, L.; Dixon, T.; Banta, R.; Ogle, I.; Dusseau, C.; Salmonson, S.; et al. Outbreak of SARS-CoV-2 B.1.617.2 (delta) variant infections among incarcerated persons in a federal prison—Texas, July–August 2021. *MMWR Morb. Mortal. Wkly. Rep.* **2021**, *70*, 1349–1354. [[CrossRef](#)] [[PubMed](#)]
5. Nishiura, H.; Ito, K.; Anzai, A.; Kobayashi, T.; Piantham, C.; Rodríguez-Morales, A.J. Relative Reproduction Number of SARS-CoV-2 Omicron (B.1.1.529) Compared with Delta Variant in South Africa. *J. Clin. Med.* **2021**, *11*, 30. [[CrossRef](#)]
6. Ito, K.; Piantham, C.; Nishiura, H. Relative instantaneous reproduction number of Omicron SARS-CoV-2 variant with respect to the Delta variant in Denmark. *J. Med. Virol.* **2022**, *94*, 2265–2268. [[CrossRef](#)]
7. Yamasoba, D.; Uriu, K.; Plianchaisuk, A.; Kosugi, Y.; Pan, L.; Zahradnik, J.; The Genotype to Phenotype Japan (G2P-Japan) Consortium; Ito, J.; Sato, K. Virological characteristics of the SARS-CoV-2 Omicron XBB. 1.16 variant. *bioRxiv* **2023**. [[CrossRef](#)]
8. Lu, Y.; Liu, D.X.; Tam, J.P. Lipid rafts are involved in SARS-CoV entry into Vero E6 cells. *Biochem. Biophys. Res. Commun.* **2008**, *369*, 344–349. [[CrossRef](#)]
9. Di Cagno, M.P. The Potential of Cyclodextrins as Novel Active Pharmaceutical Ingredients: A Short Overview. *Molecules* **2017**, *22*, 1. [[CrossRef](#)]
10. Irie, T.; Fukunaga, K.; Garwood, M.K.; Carpenter, T.O.; Pitha, J.; Pitha, J. Hydroxypropylcyclodextrins in parenteral use. II: Effects on transport and disposition of lipids in rabbit and humans. *J. Pharm. Sci.* **1992**, *81*, 524–528. [[CrossRef](#)]
11. Carpenter, T.O.; Pettifor, J.M.; Russel, R.M.; Pitha, J.; Mobarhan, S.; Ossip, M.S.; Wainer, S.; Anast, C.S. Severe Hypervitaminosis A in Siblings: Evidence of Variable Tolerance to Retinol Intake. *J. Pediatr.* **1987**, *111*, 507–512. [[CrossRef](#)] [[PubMed](#)]
12. Adorni, M.P.; Favari, E.; Ronda, N.; Granata, A.; Bellosta, S.; Arnaboldi, L.; Corsini, A.; Gatti, R.; Bernini, F. Free cholesterol alters macrophage morphology and mobility by an ABCA1 dependent mechanism. *Atherosclerosis* **2011**, *215*, 70–76. [[CrossRef](#)] [[PubMed](#)]
13. Zhang, X.; Abels, E.R.; Redzic, J.S.; Margulis, J.; Finkbeiner, S.; Breakefield, X.O. Potential transfer of polyglutamine and CAG repeat RNA in extracellular vesicles in Huntington’s disease: Background and evaluation in cell culture. *Cell. Mol. Neurobiol.* **2016**, *36*, 459–470. [[CrossRef](#)] [[PubMed](#)]
14. Hoffmann, M.; Kleine-Weber, H.; Schroeder, S.; Krüger, N.; Herrler, T.; Erichsen, S.; Schiergens, T.S.; Herrler, G.; Wu, N.H.; Nitsche, A.; et al. SARS-CoV-2 Cell Entry Depends on ACE2 and TMPRSS2 and Is Blocked by a Clinically Proven Protease Inhibitor. *Cell* **2020**, *181*, 271–280.e8. [[CrossRef](#)]
15. Yokoo, M.; Kubota, Y.; Motoyama, K.; Higashi, T.; Taniyoshi, M.; Tokumaru, H.; Tabe, Y.; Nishiyama, R.; Mochinaga, S.; Sato, A.; et al. 2-Hydroxypropyl- β -Cyclodextrin Acts as a Novel Anticancer Agent. *PLoS ONE* **2015**, *10*, e0141946. [[CrossRef](#)]
16. Palacios-Rápalo, S.N.; De Jesús-González, L.A.; Cordero-Rivera, C.D.; Farfan-Morales, C.N.; Osuna-Ramos, J.F.; Martínez-Mier, G.; Quistián-Galván, J.; Muñoz-Pérez, A.; Bernal-Dolores, V.; del Ángel, R.M.; et al. Cholesterol-Rich Lipid Rafts as Platforms for SARS-CoV-2 Entry. *Front. Immunol.* **2021**, *12*, 796855. [[CrossRef](#)]
17. Li, X.; Zhu, W.; Fan, M.; Zhang, J.; Peng, Y.; Huang, F.; Wang, N.; He, L.; Zhang, L.; Holmdahl, R.; et al. Dependence of SARS-CoV-2 infection on cholesterol-rich lipid raft and endosomal acidification. *Comput. Struct Biotechnol. J.* **2021**, *19*, 1933–1943. [[CrossRef](#)]
18. Chen, M.; Zhang, X.E. Construction and applications of SARS-CoV-2 pseudoviruses: A mini review. *Int. J. Biol. Sci.* **2021**, *17*, 1574–1580. [[CrossRef](#)]
19. Ouweneel, A.B.; Thomas, M.J.; Sorci-Thomas, M.G. The Ins and Outs of Lipid Rafts: Functions in Intracellular Cholesterol Homeostasis, Microparticles, and Cell membranes. *J. Lipid Res.* **2020**, *61*, 676–686. [[CrossRef](#)]

20. Van IJzendoorn, S.C.D.; Agnetti, J.; Gassama-Diagne, A. Mechanisms Behind the Polarized Distribution of Lipids in Epithelial Cells. *Biochim. Biophys. Acta Biomembr.* **2020**, *1862*, 183145. [CrossRef]
21. López, C.A.; De Vries, A.H.; Marrink, S.J. Molecular Mechanism of Cyclodextrin Mediated Cholesterol Extraction. *PLOS Comput. Biology* **2011**, *7*, e1002020. [CrossRef] [PubMed]
22. Clausen, T.M.; Sandoval, D.R.; Spliid, C.B.; Pihl, J.; Perrett, H.R.; Painter, C.D.; Narayanan, A.; Majowicz, S.A.; Kwong, E.M.; McVicar, R.N.; et al. SARS-CoV-2 Infection Depends on Cellular Heparan Sulfate and ACE2. *Cell* **2020**, *183*, 1043–1057. [CrossRef] [PubMed]
23. Hudák, A.; Letoha, A.; Szilák, L.; Letoha, T. Contribution of Syndecans to the Cellular Entry of SARS-CoV-2. *Int. J. Mol. Sci.* **2021**, *22*, 5336. [CrossRef] [PubMed]
24. Cantuti-Castelvetri, L.; Ojha, R.; Pedro, L.D.; Djannatian, M.; Franz, J.; Kuivanen, S.; van der Meer, F.; Kallio, K.; Kaya, T.; Anastasina, M.; et al. Neuropilin-1 facilitates SARS-CoV-2 cell entry and infectivity. *Science* **2020**, *370*, 856–860. [CrossRef]
25. Kondo, Y.; Larabee, J.L.; Gao, L.; Shi, H.; Shao, B.; Hoover, C.M.; McDaniel, J.M.; Ho, Y.; Silasi-Mansat, R.; Archer-Hartmann, S.A.; et al. L-SIGN is a receptor on liver sinusoidal endothelial cells for SARS-CoV-2 virus. *JCI Insight* **2021**, *6*, e148999. [CrossRef]
26. Wei, C.; Wan, L.; Yan, Q.; Wang, X.; Zhang, J.; Yang, X.; Zhang, Y.; Fan, C.; Li, D.; Deng, Y.; et al. HDL Scavenger Receptor B Type 1 Facilitates SARS-CoV-2 Entry. *Nat. Metab.* **2020**, *2*, 1391–1400. [CrossRef]
27. Wang, K.; Chen, W.; Zhang, Z.; Deng, Y.; Lian, J.Q.; Du, P.; Wei, D.; Zhang, Y.; Sun, X.X.; Gong, L.; et al. CD147-spike protein is a novel route for SARS-CoV-2 infection to host cells. *Signal. Transduct. Target. Ther.* **2020**, *5*, 283. [CrossRef]
28. Choudhury, A.; Mukherjee, S. In silico studies on the comparative characterization of the interactions of SARS-CoV-2 spike glycoprotein with ACE-2 receptor homologs and human TLRs. *J. Med. Virol.* **2020**, *92*, 2105–2113. [CrossRef]
29. Aleem, A.; Akbar Samad, A.B.; Sarosh, V. *Emerging Variants of SARS-CoV-2 and novel therapeutics against Coronavirus (COVID-19)*; StatPearls Publishing: Treasure Island, FL, USA, 2023. [PubMed]
30. Qu, P.; Evans, J.P.; Zheng, Y.M.; Carlin, C.; Saif, L.J.; Oltz, E.M.; Xu, K.; Gumina, R.J.; Liu, S.L. Evasion of neutralizing antibody responses by the SARS-CoV-2 BA.2.75 variant. *Cell Host Microbe* **2022**, *30*, 1518–1526. [CrossRef]
31. EMA. Background Review for Cyclodextrins Used as Excipients; 2014. Available online: http://www.ema.europa.eu/docs/en_GB/document_library/Report/2014/12/WC500177936.pdf (accessed on 18 January 2016).
32. Meredith, M.E.; Salameh, T.S.; Banks, W.A. Intranasal Delivery of Proteins and Peptides in the Treatment of Neurodegenerative Diseases. *AAPS J.* **2015**, *17*, 780–787. [CrossRef]
33. Zidovetzki, R.; Levitan, I. Use of cyclodextrins to manipulate plasma membrane cholesterol content: Evidence, misconceptions and control strategies. *Biochim. Biophys. Acta* **2007**, *1768*, 1311–1324. [CrossRef]
34. Ohvo, H.; Slotte, J.P. Cyclodextrin-mediated removal of sterols from monolayers: Effects of sterol structure and phospholipids on desorption rate. *Biochemistry* **1996**, *35*, 8018–8024. [CrossRef] [PubMed]
35. Ohtani, Y.; Irie, T.; Uekama, K.; Fukunaga, K.; Pitha, J. Differential effects of alpha-, beta- and gammacyclodextrins on human erythrocytes. *Eur. J. Biochem.* **1989**, *186*, 17–22. [CrossRef] [PubMed]
36. Papakyriakopoulou, P.; Manta, K.; Kostantini, C.; Kikionis, S.; Banella, S.; Ioannou, E.; Christodoulou, E.; Rekkas, D.M.; Dallas, P.; Vertzoni, M.; et al. Nasal powders of quercetin- β -cyclodextrin derivatives complexes with mannitol/lecithin microparticles for Nose-to-Brain delivery: In vitro and ex vivo evaluation. *Int. J. Pharm.* **2021**, *607*, 121016. [CrossRef] [PubMed]
37. Badana, A.; Chintala, M.; Varikuti, G.; Pudi, N.; Kumari, S.; Kappala, V.R.; Malla, R.R. Lipid Raft Integrity Is Required for Survival of Triple Negative Breast Cancer Cells. *J. Breast Cancer* **2016**, *19*, 372–384. [CrossRef] [PubMed]
38. Lichtenhan, J.T.; Hirose, K.; Buchman, C.A.; Duncan, R.K.; Salt, A.N. Direct administration of 2-Hydroxypropyl-beta-cyclodextrin into guinea pig cochlea: Effects on physiological and histological measurements. *PLoS ONE* **2017**, *1*, e0175236. [CrossRef]
39. Bezerra, B.B.; Silva, G.P.D.D.; Coelho, S.V.A.; Correa, I.A.; Souza, M.R.M.; Macedo, K.V.G.; Matos, B.M.; Tanuri, A.; Matassoli, F.L.; Costa, L.J.D.; et al. Hydroxypropyl-beta-cyclodextrin (HP-BCD) inhibits SARS-CoV-2 replication and virus-induced inflammatory cytokines. *Antivir. Res.* **2022**, *205*, 105373. [CrossRef]

Disclaimer/Publisher’s Note: The statements, opinions and data contained in all publications are solely those of the individual author(s) and contributor(s) and not of MDPI and/or the editor(s). MDPI and/or the editor(s) disclaim responsibility for any injury to people or property resulting from any ideas, methods, instructions or products referred to in the content.